Procedure for a detailed territorial assessment of wind-driven rain and driving-rain wind pressure and its implementation to three Spanish regions

José M. Pérez-Bella[a], Javier Domínguez-Hernández[a,*], Enrique Cano-Suñén[a], Juan J. del Coz-Díaz[b], Ángel Martín-Rodríguez[b]

[a] *Department of Construction Engineering, Engineering and Architecture School, University of Zaragoza (UZ), María de Luna, s/n, 50018, Zaragoza, Spain*

[b] *Department of Construction Engineering, University of Oviedo, Edificio Departamental Viesques nº 7, 33204 Gijón, Spain.*

Abstract

Wind-driven rain and the simultaneous action of wind pressure contribute to water penetration into building façades. Therefore, both climatic parameters must be considered in the design of building enclosures to manage the effects of water intrusion. This article presents a procedure for determining both parameters in a geographic area, by combining various data sources. The procedure was implemented in three Spanish regions with different climates (Galicia, Catalonia and Andalusia), by combining precipitation and wind velocity records compiled at 393 weather stations distributed across these regions, using wind maps, and fitting relationships between exposure indices. In comparison to other studies, this procedure allows for data from a relatively large number of locations to be included in the exposure assessment, which can produce a more detailed characterisation across the territory and facilitate the creation of isopleth exposure maps. A risk index of water penetration, which combines the influence of both exposures, was also calculated. The results showed that the exposure of building façades to water penetration was driven by the climate of each zone. Galicia is the most exposed region. Moreover, the Strait of Gibraltar and Gulf of Cadiz in Andalusia and the Cape of Creus in Catalonia are also zones of high exposure.

Keywords

Driving rain; Wind pressure; Weather observations; Building design; Isopleth maps; Spain

[*] Corresponding author. Department of Construction Engineering, University of Zaragoza (UZ), María de Luna, s/n, 50018, Zaragoza, Spain. Tel.Fax: +34 976 76 21 00.
E-mail address: javdom@unizar.es (Javier Domínguez-Hernández)

1. Introduction

The simultaneous action of precipitation and wind pressure on building façades leads to wetting of construction materials and penetration of atmospheric water into building enclosures (Blocken and Carmeliet, 2004; Blocken et al., 2013). Wind action on raindrops imparts a horizontal component to their fall velocity, causing them to impinge the exterior surface of building walls (wind-driven rain or WDR). Simultaneously, wind pressure acting on a building façade (driving rain wind pressure or DRWP) facilitates water penetration through the pores and cracks present in the building façade.

Therefore, exposure to the combined action of WDR and DRWP is considered to be the primary cause for problems associated with water penetration into building components above ground (Sahal and Lacasse, 2004; Cornick and Lacasse, 2005; Kerr, 2004), including reduced thermal performance and subsequent increases in energy consumption (del Coz et al., 2013; Sanders, 1996), increased maintenance costs (Franke et al., 1998; Waldrum, 1993; Tang, 2004), and even health problems for building residents (Haverinen, 2007; WHO, 2011). Characterising the exposure to both climatic parameters for a given location is therefore a primary goal when designing building enclosures that minimise these problems (Carll, 2001; Kvande and Lisø, 2009; Straube and Burnett, 1999).

Many studies in different countries have focused on the analysis of WDR exposure (Blocken and Carmeliet, 2004). These studies analysed this exposure for a discrete number of locations distributed throughout a particular geographic area, e.g., 1 location per 26,000 km^2 in Chile and Nigeria (Pérez et al., 2013a; Akingbade, 2004); 1 location per 9,400 km^2 in India (Chand and Bhargava, 2002); 1 location per 4,250 km^2 in Greece (Giarma and Aravantinos, 2011); or 1 location per 3,300 km^2 in Turkey (Sahal, 2006).

However, the representativeness of these exposure results is limited in areas that are distant from the locations for which the exposure was determined. According to the international standard ISO 15927-32009 (ISO, 2009), the validity of exposure results can be extended to locations within a maximum radius of 100 km around the location for which WDR exposure is known (for flat regions with differences in height less than 100 m). In mountainous or hilly regions or in coastal and lakeside areas, the validity radius is likely considerably smaller. These limitations mean that the results of the analyses typically performed to extract WDR conditions are only reliable close to the analysed locations, leaving extensive areas without a valid estimate of WDR exposure.

In most countries, estimating this exposure at additional locations is limited by the number of available weather stations that have concurrent records of rain and wind of sufficient age and precision. To the best of the authors' knowledge, only the United Kingdom has attempted to estimate WDR exposure in a detailed way throughout its entire territory using wind patterns and precipitation records to interpolate the values of WDR exposure in areas located far from the analysed sites (BSI, 1992; Prior, 1985).

This study proposes an alternative procedure that permits analysing a large number of additional locations by combining rainfall records and wind velocity data, gathered at weather stations, with information from regional wind maps and fitting relationships between different exposure indices. As a demonstration, the procedure was applied to generate a detailed estimate of the WDR and DRWP exposures in three regions of Spain: Galicia (1 location per 370 km^2), Catalonia (1 location per 218 km^2) and Andalusia (1 location per 525 km^2). This allowed for the characterisation of the entire territory encompassing these regions through the creation of different isopleths exposure maps. The WDR and DRWP exposure values obtained in these regions also allowed for the calculation of a detailed risk index of water penetration, or RIWP (Pérez et al., 2013b), that characterises the combined effect of both exposures on building façades.

2. Background

The characterisation of the two exposures (WDR and DRWP) is necessary to adequately determine the risk of water penetration through a building façade. A number of investigations have shown that driving rain is capable of penetrating deteriorated façades (walls with pores and cracks larger than 5 mm) even in the absence of significant wind pressure (Cornick and Lacasse, 2005; Sahal and Lacasse, 2004). Likewise, a relatively small quantity of driving rain can penetrate building enclosures without defects or pores greater than 1 mm if elevated wind pressure occurs simultaneously with rain deposition on the building façade. Due to the variety of surface finishes and different states of building maintenance, both climatic parameters must be considered to develop a comprehensive characterisation of water penetration risk in building façades.

Although there are currently different procedures that can be used to quantify each parameter with great precision, it is preferable to use simple and functional calculation methods to determine these exposures at many locations using a reasonable effort. Therefore, the majority of studies on WDR have used semi-empirical calculation methods based on the "WDR relationship" (Hoppestad, 1955; Lacy, 1965).

Compared to more precise CFD methods, which require extensive datasets to define each situation (Blocken et al., 2011a, 2011b; Hensen and Lambert, 2011; Kubilay et al., 2013), the WDR relationship can be used to approximately determine the WDR exposure based on climatic data that are generally recorded at a majority of weather stations irrespective of the country of interest. Thus, the WDR value (l/m^2) may be estimated based on records of precipitation intensity R_h (l/m^2) for each precipitation event at a given location and wind velocity U (m/s) occurring simultaneously at the same location by applying the empirically fitted coefficient k (s/m) of Eq. 1:

$$WDR = k \cdot U \cdot R_h \tag{1}$$

The fitted coefficient k (physically related to the terminal falling velocity of raindrops) is affected by the characteristic size of water droplets for each precipitation event and, therefore, also influenced by the

rainfall intensity. Various studies have proposed mean values for this coefficient, which may range between 0.20 and 0.25 s/m (Lacy, 1977; Straube and Burnett, 2000).

However, the simplest and most widespread application of the WDR relationship does not use a fitted coefficient. Instead, it considers a driving rain index (DRI), which is used to qualitatively characterize WDR exposure independent of location-specific storm events (Lacy and Shellard, 1962). This scalar index (m^2/s), which is typically averaged over an annual period (*aDRI*), can be calculated using average annual records (*aaDRI*) for precipitation R_h (mm/year) and wind velocity U (m/s) gathered over N years at each sampling location (Eq. 2). The velocity records are usually taken under reference conditions, i.e., at a height of 10 m over clear and obstacle-free terrain (WMO, 2008).

$$aaDRI = \frac{\sum_{i=1}^{N} U \cdot \left(R_h \diagup 1000 \right)}{N} \tag{2}$$

The use of monthly or daily averaged values (*maDRI* and *daDRI*, *respectively*) reduces data averaging and co-occurrence errors (Blocken and Carmeliet, 2007, 2008). While this scalar index does not quantify the volume of driving rain or its distribution along different building wall orientations, it does provide an exposure estimate, and it has been shown by Henriques (1992) that an empirical fit can be used to relate the index value with a WDR estimation (l/m^2).

Moreover, a scalar calculation based on climatic records gathered at each site can be used to determine the DRWP exposure value (Cornick and Lacasse, 2005). Therefore, the mean driving rain wind pressure $DRWP_a$ (Pa) value may be obtained using the Bernoulli equation (Eq.3), where C_p represents a pressure coefficient (usually equal to 1), ρ_{air} (kg/m^3) represents air density and U (m/s) represents wind velocity at the time of a significant precipitation event (>0.05 mm). To determine the mean wind pressure, m records of simultaneous wind and rain events gathered over multiple years can be averaged.

$$DRWP_a = \frac{\sum_{i=1}^{m} C_p \cdot \frac{1}{2} \cdot \rho_{air\ i} \cdot U_i^{\ 2}}{m} \quad (3)$$

Similar to the *aDRI* index, the wind velocity records typically refer to reference conditions, i.e., DRWP exposure is calculated at a height of 10 m over clear and obstacle-free terrain. Moreover, the use of wind records collected over shorter time intervals allows for consideration of only those wind velocity records that occur simultaneously with rainfall, thereby reducing co-occurrence errors in the calculation of DRWP exposure.

As discussed above, the precision of both indices (*aDRI* and $DRWP_a$) depends on the quality of available climatic records. In contrast, the level of detail for the WDR and DRWP exposure analysis performed for a geographic area depends on the distance between sampling locations for the data used in the calculation (i.e., the number of points analysed).

2.1 Previous studies conducted in Spain

Several studies have been conducted to generally characterise WDR and DRWP exposures in Spain by analysing climatic data gathered over 30 years at 80 locations (Pérez et al., 2012, 2013b, 2013c). These studies have provided a level of precision higher than typically attained in other countries because they used daily climatic records of precipitation and wind velocity rather than monthly or annual records often used in other countries (Akingbade, 2004; Chand and Bhargava, 2002; Giarma and Aravantinos, 2011; Sahal, 2006).

Nevertheless, at the scale of 1 result per 6,300 km^2, these studies are not sufficient to obtain a representative characterisation of the entire Spanish territory, especially for areas far from urban centres. This effect is compounded by the mountainous topography in the country, which drastically reduces the validity range of the exposure indices obtained from those locations forming part of the study.

Only 22 of the 80 locations used in these studies corresponded to the three regions of interest in this paper: 5 locations in Galicia, 5 in Catalonia and 12 in Andalusia (see Table 1). Therefore, the coverage of exposure estimates for these three regions is insufficient (1 location per 6,770 km^2) and the distribution of exposure estimates is also irregular, with the 22 locations being concentrated in large coastal cities or zones at altitudes lower than its surroundings (see Fig. 1).

Figure 1. Map of Spain illustrating the location of the three regions of interest for analysis and the locations in these regions considered in previous studies (Pérez et al., 2012, 2013b, 2013c). *Darker colours represent higher altitudes*.

This study is supported by prior research and proposes a procedure that increases the number of locations that can be considered for exposure analysis, thus improving the coverage of estimates of both exposure indices for the area being studied. An additional 371 analysis points in the three regions were combined with the 22 previously analysed sites (for a total of 393 locations). The new data were provided by the regional meteorological agencies that manage a larger number of stations in its territory as compared to that managed by the Spanish Meteorological Agency (see Table 1).

Table 1.

Comparison of terrain coverage from previous studies in Spain (Pérez et al., 2012, 2013b, 2013c) and the coverage of the current study.

To calculate the exposure indices, the mean precipitation and wind records (usually monthly) collected from weather stations at the locations mentioned above were analysed. Wind velocity data for the locations (which were incomplete or non-existent in many cases) were supplemented with wind velocity estimates derived from available wind maps (IDAE, 2009). Finally, different fitting relationships were identified and used to build more precise WDR and DRWP exposure indices than those derived from the monthly climatic data available at many stations.

Due to the large number of locations included in the analysis, the distance between analysed points was less than that of previous studies. This allowed for a more detailed analysis of the entire geographic area because the large number of data points reduced the uncertainty associated with the interpolation of exposure results. Therefore, rather than producing a typical exposure map representing the results at a limited number of locations, in this study detailed isopleths maps are presented. The combination of climatic records and information derived from wind maps and the treatment of these data using fitting relationships may be used in different countries or regions where the nature of the topography or a reduced number of stations with adequate climatic records precludes the characterisation of broad zones.

3. Procedure for detailed exposure analysis in three regions of Spain

To increase the number of locations for the analysis and improve the characterisation of WDR and DRWP exposures, a procedure that combines three components is presented: precipitation and wind velocity records collected at weather stations, regional maps of wind velocity and fitting relationships between different exposure indices.

Figure 2. Scheme for the combination of the data sources to undertake a detailed analysis of WDR and DRWP exposures.

Climatic records

A detailed evaluation of exposure conditions (see Eqs. 2 and 3) requires an initial analysis of climatic records for precipitation and wind that gathered from a large set of locations in the geographic area of interest. The procedure used here is based on these climatic records. However, they are supplemented by additional data sources to improve the precision of the results.

This study used climatic records from 371 additional pluviometric stations provided by the regional governments of Galicia, Catalonia, and Andalusia (Genelatitat of Catalonia, 2013; Junta of Andalusia, 2013; Xunta of Galicia, 2013). For the regions of Galicia and Catalonia, the data included monthly summaries for precipitation and occasionally also data for mean wind velocity. In Andalusia, daily records for both precipitation and wind velocity were available from the majority of sampling locations.

All records were collected after 1997 and were between 2 and 10 years old. The average precipitation in the years of available data is similar to the historical average for the country (AEMET, 2013). Therefore, the resulting estimates of WDR exposure can be considered characteristic of the country's conditions (between 2004 and 2012, recorded precipitation values reached 96% of the mean value for the 1971-2000 historical data series).

Wind maps

Despite the fact that Spain has a large number of pluviometric stations distributed across their territory, wind velocity records are typically much less common, or have been gathered in a discontinuous fashion, or are only available for recent years. This lack of wind velocity data prevented the calculation of the *aDRI* and $DRWP_a$ indices at many of the locations, thereby limiting the number of results when conducting the analysis.

At sites that lack wind records, have incomplete data, or have less than 2 years of records, the procedure used in this study draws on an alternative source of data to estimate the mean wind velocity. Wind maps completed for statistical purposes by different national or regional meteorological agencies and wind maps created for wind energy development may be used.

The mean wind velocity derived from these maps may be used as a constant value U (m/s) in Eq. 2 to approximate the *aDRI* index for locations with incomplete data, increasing the number of points where the WDR exposure can be estimated. Because this mean wind velocity does not account for the simultaneity with precipitation events, the Eq. 3 only determines wind pressure at a given location and not DRWP exposure.

Some of the 371 new stations did not have monthly or daily mean values for the wind velocity that corresponded with precipitation records during the same time period. Some stations only had rainfall records (19 stations in Galicia and 8 in Catalonia), whereas at other sites, more years of data were available for precipitation than for wind or there were temporal gaps in wind records.

To include these stations in the analysis of WDR and DRWP exposures, the historical data series for wind at each station was completed using available wind maps, developed using a numerical model (Mesoscale Atmospheric Simulation System). This model has been validated through more than 10 years of use and uses geophysical and meteorological reanalysis databases, rawinsonde data, and climatic records from surface stations (IDAE, 2009). These maps provide mean wind velocity estimates at an altitude of 80 m above the ground surface and are used in the development of wind power production in the three regions of Spain. Their relatively high-resolution data (100 m grid) allowed for the precise determination of mean wind velocities at the location of each weather station for which there was incomplete wind data. These mean wind velocities can supplement the incomplete data by replacing the nonexistent monthly or daily data.

To determine wind velocity under reference conditions (at an altitude of 10 m above the ground surface), the wind profile power-law can be used, where the wind velocity U_{10} (m/s) at a height of 10 m is calculated using the known wind velocity U_Z (m/s) at altitude z (m) (in this case, 80 m) (Eq. 4). The parameter α represents a friction coefficient derived from the surrounding terrain and frequently assumed to be 1/7 for open fields without obstacles (Bansal et al., 2002).

$$U_{10} = \frac{U_Z}{\left(\frac{z}{10}\right)^{\alpha}} \tag{4}$$

In Galicia and Catalonia, the combination of monthly precipitation records R_h (mm) and wind velocity records (obtained from weather stations or derived from wind maps) allowed Eq. 2 to be used to obtain the *maDRI* index for each station. However, this method is not as precise as the results obtained from previously conducted studies in Spain based on daily weather data (Pérez et al., 2012, 2013b, 2013c), and it does not allow for determining $DRWP_a$ without a large co-occurrence error. In Andalusia, the availability of daily precipitation data and wind records (sometimes supplemented with mean values from wind maps) allowed for calculating the *daDRI* index using Eq. 2 to obtain a similar level of precision to that obtained from these previous studies.

Fitting relationships

Numerous studies have identified the relationships among *daDRI*, *maDRI* and *aaDRI* for various locations (Akingbade, 2004; Chand and Bhargava, 2002; Giarma and Aravantinos, 2011; Pérez et al., 2012; 2013a), which has led to the definition of general relationships that can be extrapolated to other locations within the same zone. The use of these relationships allows for estimating more precise index values (e.g., *daDRI*) using indices determined at locations with limited climatic records (e.g., *maDRI* values calculated using mean monthly precipitation and wind velocity).

Therefore, to estimate the WDR exposure in Galicia and Catalonia to a similar precision as that which could be obtained using daily weather data, the fitting relationship that relate the *maDRI* and *daDRI* values at the locations must be calculated. Prior studies conducted in Spain have already presented a general *daDRI-maDRI* relationship based on results from locations distributed in the country (Pérez et al., 2012). However, it is expected that using more representative relationships of the specific climatic conditions in the regions of interest will yield more accurate results. Therefore, only the *daDRI* and *maDRI* results located in the two regions without new daily records have been selected from these prior studies (5 in Galicia and 5 in Catalonia). Because of the age and reliability of the records in those studies (over 30 years of daily records were used), the *daDRI-maDRI* relationships obtained for Galicia (Eq. 5) and Catalonia (Eq. 6) could be extrapolated to the remaining stations in both regions.

$$daDRI_{Galicia} = 1.2024 \cdot maDRI_{Galicia} - 0.1132 \quad (5)$$

$$daDRI_{Catalonia} = 1.1873 \cdot maDRI_{Catalonia} - 0.2111 \quad (6)$$

The two best-fit linear relationships between *maDRI* and *daDRI* and the general relationship previously determined for the entire country are represented in Fig. 3. Despite the relatively low number of available points in both regions, all of the fitted models are represented by similar expressions and have large coefficients of determination (R^2), especially for Catalonia.

After calculating the *maDRI* values for each of the stations in Galicia and Catalonia, Eqs. 5 and 6 can be used to estimate the *daDRI* exposure index at each location. Therefore, the WDR exposure can be estimated with similar precision to the determination of the WDR for Andalusia, where *daDRI* was directly calculated based on the daily climatic data records available at stations in the region.

Figure 3. Best-fit linear *maDRI-daDRI* relationships derived from the results of previous studies (Pérez et al., 2012).

Eq. 3 can be used to calculate the DRWP exposure using only wind velocity data that correspond to events during which significant precipitation occurs. This distinction could only be established with reasonable precision in the case of Andalusia where wind records were discarded on days without precipitation due to the availability of daily climatic data.

In contrast, the monthly mean wind data available from stations in Galicia and Catalonia did not allow for the above distinction. Therefore, Eq. 3 only provides a mean value of wind pressure for each location. To estimate $DRWP_a$ with a precision comparable to the estimates for Andalusia, it is necessary to determine new fitting relationships using accurate results available from prior studies in some locations of both regions (Pérez et al., 2013b, 2013c).

$DRWP_a$ values that were previously calculated using daily records from stations in Galicia and Catalonia were related to the mean wind pressure at the corresponding locations to identify representative fitting relationships for each region (Eqs. 7 and 8). Thus, the mean wind pressures obtained for the locations can be used to estimate more precise $DRWP_a$ values similar to those that would have been obtained based on daily wind velocity and precipitation data.

$$DRWP_{\text{a }Galicia} = 1.2919 \cdot mean\ wind\ pressure_{Galicia} - 0.3530 \quad (7)$$

$$DRWP_{\text{a }Catalonia} = 0.9554 \cdot mean\ wind\ pressure_{Catalonia} - 0.4926 \quad (8)$$

Both Eqs. 7 and 8 have large coefficients of determination, as was for the previous *daDRI-maDRI* relationships. In this case, the R^2 value is greater for the region of Galicia. Fig. 4 shows the equations described above and the general relationship for the entire country, which was derived based on data from previous studies (Pérez et al., 2013b, 2013c). Similar to the other fitting relationships described above, the equations for the two regions had higher coefficients of determination than the relationship for the entire

country. In Catalonia, the driving rain wind pressure was slightly lower than the mean wind pressure. In Galicia, the situation was reversed.

Figure 4. Best-fit linear *$DRWP_a$-mean wind pressure* relationships derived from the results of previous studies (Pérez et al., 2013b, 2013c).

Combining climatic records, wind maps, and fitted relationships (see Fig. 5) allows for a detailed characterisation of WDR and DRWP exposures in the analysed Spanish regions. An increased number of locations were included in the analysis compared to previous studies. The procedure also resulted in a similar degree of precision than obtained from daily records of wind and precipitation.

Figure 5. Integration of climatic data, wind maps and fitting relationships using the procedure described in this study.

3.1 Risk index of water penetration

The *daDRI* and *$DRWP_a$* exposure indices obtained for each of the locations included in the study were used to determine the Risk Index of Water Penetration (RIWP) through building façades, which accounts for the combined influence of both parameters on water penetration into building enclosures (Pérez et al., 2013b). To calculate this index, the exposure results for each location *j* can be normalised based on the maximum and minimum values in the sample (Eqs. 9 and 10).

$$daDRI_{normalised\ j} = \frac{daDRI_j - daDRI_{\min}}{daDRI_{\max} - daDRI_{\min}} \quad (9)$$

$$DRWP_{a\ normalised\ j} = \frac{DRWP_{a\,j} - DRWP_{a\min}}{DRWP_{a\max} - DRWP_{a\min}} \quad (10)$$

Finally, these normalised values (which fall between 0 and 1) are combined into a unique index for each location using Eq. 11. The greater the normalised value is, the greater is the combined risk index. In this calculation, it is assumed that both parameters (i.e., *daDRI* and $DRWP_a$) have equal influence on the water penetration process through building façades, although weighting factors can be added to represent the relative influence of each parameter according to the surface finish of the enclosure (Pérez et al., 2013a; 2013b).

$$RIWP_j = \sqrt{\left(daDRI_{normalised\ j}\right)^2 + \left(DRWP_{\text{a}\ normalised\ j}\right)^2} \quad (11)$$

To determine the *RIWP* index for locations in the three regions of interest, the *daDRI* and $DRWP_a$ values were normalised by considering the range of exposure results from the 393 available sites. Thus, 22.5 m^2/s (Lousame, Galicia) was considered the maximum value for exposure to driving rain ($daDRI_{max}$), whereas 0.1 m^2/s (Alcarrás, Catalonia) was considered the minimum $daDRI_{min}$ value. The maximum $DRWP_{a\,max}$ was 55.0 Pa (Tarifa, Andalusia), whereas the minimum $DRWP_{a\,max}$ value was 0.1 Pa (Orcera, Andalusia).

This characterisation allows for a comprehensive comparison of exposures between different sites and establishes shared risk ranges for the three regions. This unique index can be used to design building enclosures that will guarantee the water tightness for each risk range.

In the next section, the most relevant results for WDR and DRWP exposures and the most significant *RIWP* values for each of the three regions are discussed. Finally, a detailed characterisation of these

indices throughout the territory is presented through the elaboration of isopleths maps specific to each region.

3.2 Exposure results in Galicia

Galicia is located at the North-western end of the Iberian Peninsula (North of Portugal) and is bordered by the Atlantic on its northern and western boundaries (see Fig. 1). The influence of the ocean gives the region an oceanic climate, which is combined with a warm-summer Mediterranean climate (Kottek et al., 2006). The topography is characterised by mountains and low hills, which are more abrupt in the southeast, where they reach an altitude of 2,100 m. Along the coast there are several firth-like inlets (also named rias). The main cities are concentrated along the west coast (e.g., Vigo and La Coruña) and in the provincial capitals. However, other population centres are evenly distributed throughout the entire region.

To analyse the entire region (29,575 km^2), 80 weather stations were considered and these were located at elevations ranging from as low as 2 m above sea level (Cíes Islands, on the south western coast) to a height of 1,302 m in O Cebreiro (at the eastern edge of the region). The 80 stations were uniformly distributed across the region, with a minimum distance between locations of 2.6 km (between the Vilela and Vilamaior stations in the Verín municipality) and a maximum distance of 25 km. Thus, the areal coverage was approximately one station per every 370 km^2.

The calculation procedure shown at the beginning of this section was used to obtain the *daDRI* and $DRWP_a$ indices for each location based on monthly climatic records. The estimated wind velocity was based on available wind maps for the region and the results were fitted using Eqs. 5 and 7 to obtain more precise exposure indices.

The results were also used to determine the combined *RIWP*. Table 2 shows the results for stations at which the combination of the two exposure parameters (WDR and DRWP) generated a higher risk index of water penetration.

Table 2.

Weather stations in Galicia with a risk index of water penetration greater than 0.4 (*31 of the 80 total stations*).

Figs. 6 and 7 show the isopleth maps representing the WDR and DRWP exposure values associated with each point in the region. A linear interpolation of the indices obtained for each location was used to generate smoothed isopleths representing the exposure on these maps. The short distance between the locations used in this study (compared to previous studies in Spain and other countries) resulted in a significant reduction in the uncertainty of the interpolated results.

Figure 6. *daDRI* isopleth map of Galicia, Spain (m^2/s).

In general, the entire region has high WDR exposure, which corresponded with its coastal setting characterised by strong Atlantic winds and elevated precipitation. Exposure is higher on the western coast where the incidence of these winds is greater. Thus, the high value of *daDRI* reached 22.5 m^2/s in Lousame and 18.2 m^2/s in Cuntis. WDR exposure decreased toward the North and East, with "protected" areas showing exposure values lower than 3 m^2/s (Lacy, 1971).

Figure 7. $DRWP_a$ isopleth map of Galicia, Spain (Pa).

Driving rain wind pressure is also high in this region, especially on the coast where values lower than 10 Pa are rarely observed. The Northern location of Cedeira has the highest $DRWP_a$ value (46.7 Pa), followed by Lousame and Cuntis, with values of 37.2 and 35.9 Pa, respectively. In the interior, the distribution of values for DRWP exposure is irregular (due to the topography) with DRWP exposure reaching above 25 Pa in locations that include Cabeza de Manzaneda, A Veiga or Rodeiro.

In both maps it is clear that exposure values from previous studies for some locations (e.g., Santiago airport, Vigo airport, La Coruña airport, La Coruña and Pontevedra) are consistent with the pattern of isopleth derived from the new locations. Despite the fact that the previous values were calculated based on daily weather data recorded over 30 years, the points (represented on the maps with a different "△" symbol) are well-integrated into the results of the new procedure. The results near these locations show that the proposed procedure can provide suitable estimates of the exposures, reinforcing its validity.

3.3 Exposure results in Catalonia

Catalonia has a surface area of 32,105 km^2 and is located in the extreme North-eastern region of the country, bordered by France to the North and the Mediterranean Sea to the East and South. The influence of the sea and the high-elevation Pyrenees to the North results in the combination of different climates within the region, including a Mediterranean climate and a mountain climate (Kottek et al., 2006). The highest peaks are located in the Pyrenees, reaching elevations of 3,140 m. However, along the coast there are also alternating plains and mountains that can reach altitudes of 1,700 m. Between these two mountain ranges (in the central and Western parts of Catalonia), there is a broad depression formed by high plateaus that decrease in altitude to the southwest.

The primary inhabited areas are concentrated on the coast (e.g., Barcelona and Tarragona). However, there are population centres distributed across the interior, such as the city of Lleida (located in the

western part of the region). The distribution of the 147 weather stations included in this region followed the same pattern as the distribution of population centres, with weather stations concentrated in the coastal areas and decreasing in density to the northwest. The average coverage was one station per 218 km^2; along the coast this value was even lower. The altitude of the stations varied from sea level at the Ebro Delta station to over 1,950 m in Queralbs (to the North, near the border with France).

Table 3 shows the *daDRI* and $DRWP_a$ results and the combined risk index of water penetration (*RIWP*) obtained for the stations with a risk index of water penetration greater than 0.15. For the majority of these locations, the exposure to water penetration of building façades is much lower than the exposure levels in Galicia.

Table 3.

Weather stations in Catalonia with a risk index of water penetration greater than 0.15 (*16 of the 147 total stations*).

Following the same procedure used to create the maps for Galicia, Fig. 8 shows the WDR exposure associated with each zone of the region using *daDRI* isopleths. Similar to the results for Galicia, the large number of analysed points allows for a comprehensive characterisation of the entire region by interpolating between exposure results. As shown in Fig. 8, the region can be considered as "protected" (i.e., *daDRI*<3 m^2/s), except in the area in proximity to the Cape of Creus. The highest exposure value was for Portbou (5.1 m^2/s). In the interior, large areas show a negligible level of exposure (lower than 1 m^2/s).

Figure 8. *daDRI* isopleth map of Catalonia, Spain (m^2/s).

The higher WDR exposure in Portbou can be explained by the higher driving rain wind pressure in the area surrounding the Cape of Creus (see Fig. 9). Generally, the majority of locations show very low $DRWP_a$ values, lower than 5 Pa. Overall, the degree of exposure is noticeably lower than that in Galicia. As might be expected, the presence of coastal winds results in higher wind pressures at some stations close to the coast.

Figure 9. $DRWP_a$ isopleth map of Catalonia, Spain (Pa).

The *RIWP* indices for the region are much lower than those obtained for Galicia (only Portbou shows a *RIWP* value greater than 0.3). Similarly as was obtained for the Galicia region, the exposure values obtained from previous studies for the Barcelona airport, the Gerona airport, Lleida, the Reus airport and Tortosa are consistent with the isopleth configuration on the maps, thereby reinforcing the validity of the procedure used in this study.

3.4 Exposure results in Andalusia

Andalusia has a greater surface than that the combined areas of Galicia and Catalonia combined (87,270 km^2) and comprises all of southern Spain. It is bordered by Portugal and the Atlantic Ocean to the west and southwest, respectively, and the Mediterranean Sea to the south and southeast. There is significant variation in altitude throughout the region, including two large mountain ranges: the Sierra Morena (in the North), with mountains reaching 1,300 m, and the Baetic System (parallel to the southern and southeastern coasts), with heights up to 3,475 m. Between both mountain ranges is the Baetic Depression, that has altitudes below 250 m; the depression follows the Guadalquivir River down to its mouth at the

Atlantic Ocean. These varied topographical conditions results in diverse climates (the mean annual precipitation generally decreases from West to East in this region). The Mediterranean climate predominates, but desert and mountain climates can also be identified (Kottek et al., 2006).

The population centres are primarily concentrated in the Baetic Depression (e.g., Seville, Cordoba and Jerez de la Frontera) and along the southern coast (e.g., Malaga and Almeria). In the mountainous regions, only the provincial capitals (Granada and Jaen) have significant population concentrations. However, as in the other two regions, there are uniformly-distributed population centres throughout this region.

Unlike Galicia and Catalonia, daily records were available for the analysis in this region to directly obtain the *daDRI* and $DRWP_a$ indices, without the use of fitting relationships. In the analysis of this region, 166 weather stations were considered that were uniformly distributed across the region, except in the Sierra Morena area (to the North) and the Eastern portion of the region, where the density of stations was noticeably lower. On average, there was 1 station per 525 km^2. Together, the stations covered altitudes ranging from sea level (at the coastal population centres) to 1,700 m in Castellar de Santisteban (North-eastern part of Andalusia).

Table 4 shows the exposure values associated with locations with a greater risk of water penetration (*RIWP* value greater than 0.2). While there are some locations with significant WDR and DRWP exposures, many locations (154 of 166) were characterised by relatively low values for this risk index.

Table 4.

Weather stations in Andalusia with a risk index of water penetration greater than 0.2 (*12 of the 166 total stations*).

Figs. 10 and 11 are the respective isopleth maps of WDR and DRWP exposures for the region of Andalusia. Fig. 10 shows elevated driving rain exposure in areas close to the Strait of Gibraltar (San Roque, 7.9 m^2/s), whereas the remainder of the region has *daDRI* values below 3 m^2/s. Generally, lower values of WDR exposure are found in the eastern portion of Andalusia due to the lower precipitation rates prevalent in that area.

Figure 10. *daDRI* isopleth map of Andalusia, Spain (m^2/s).

Fig. 11 shows higher driving rain wind pressure in certain coastal cities. The $DRWP_a$ values for the Strait of Gibraltar and the Atlantic coast are especially significant. In these areas, the influence of Atlantic winds results in a higher degree of exposure in certain coastal cities including Moguer, Cadiz and Tarifa. The exposure also becomes progressively lower in settlements located towards the interior of the Baetic Depression (Jerez de la Frontera, Moron de la Frontera, Seville and Cordoba). Nonetheless, the $DRWP_a$ values for the entire region are mostly below 5 Pa.

Figure 11. $DRWP_a$ isopleth map of Andalusia, Spain (Pa).

4. Discussion

Comparing the results for the three regions, overall, Galicia had higher exposures compared with Catalonia and Andalusia, where only some locations showed high exposure values. These results are consistent with those obtained from prior studies conducted in Spain (Pérez et al., 2012; Pérez et al.,

2013b, 2013c) in which the North-western Iberian Peninsula and the Gulf of Cadiz area were identified as the regions with the least favourable climatic conditions for building façades.

It was not possible to identify a correlation between the WDR exposure index and driving rain wind pressure in any of the regions. Andalusia, which had the highest $DRWP_a$ value (Tarifa, 55.0 Pa), and with generally lower levels of *daDRI*, had a particularly low coefficient of determination R^2 (see Fig. 12). This finding reinforces the fact that the use of one parameter alone (typically the WDR exposure in most countries) is not sufficient to adequately evaluate comprehensive exposure risk for buildings with regard to atmospheric water penetration.

Figure 12. Best-fit linear *WDR-*$DRWP_a$ relationships in Galicia, Catalonia and Andalusia.

Fig. 13 shows an isopleth map that represents the *RIWP*, which integrates the two climatic parameters into one indicator of water penetration risk in building façades, for the three regions of interest in this study. The map represents a qualitative and consistent characterisation of this risk for these regions. This type of map provides a useful complement for the partial characterisation of exposure conditions obtained from the WDR and DRWP isopleth maps.

Figure 13. Risk index of water penetration in building façades for the three Spanish regions.

Galicia also showed a greater overall risk of atmospheric water penetration in comparison to other regions. In Catalonia and Andalusia, the value of *RIWP* surpassed 0.2 in certain zones, but almost the

entire territory of Galicia showed index values above this threshold. The west coast of Galicia (*RIWP*>1.2), the Strait of Gibraltar (*RIWP*>1.0) and the Gulf of Cadiz coast (*RIWP*>0.4) in Andalusia, and the northeast edge of Catalonia (*RIWP*>0.6) were the most exposed areas of the three regions analysed in this study.

Combined information from the risk index of water penetration and the WDR and DRWP exposures in the three regions may help in the design of building façades to manage different environmental conditions and can be a useful tool for the creation of policy guidelines that limit or prevent water penetration into buildings. This detailed analysis for a geographic area could be used to improve façade designs at any site, even those located far from primary weather stations or large urban centres.

5. Conclusions

This article demonstrates the use of a procedure for determining the WDR and DRWP exposures using combined data from different sources (daily or monthly climatic records obtained from weather stations, regional wind maps, and fitting relationships for various exposure indices). Through the application of this procedure, the exposure of building façades to atmospheric water penetration was determined for 393 locations distributed across three Spanish regions: Galicia, Catalonia and Andalusia. These WDR and DRWP exposure values were combined to calculate a risk index of water penetration, which combines both parameters into a single indicator.

The method for combining different sources of data may also be applicable in other countries where the nature of the topography or the limited number of locations with adequate climate data impede a comprehensive characterisation of these exposures across the territory. Compared to prior studies, the combination of data sources in this study resulted in an increased number of locations with useable climate data, thereby reducing the spatial distance between exposure estimates and the uncertainty

inherent to the interpolation of exposure values between these data points. Therefore, various exposure and risk isopleth maps can be created to provide a detailed coverage of any geographic area. This method can be used to improve the design of building façades at any location.

Compared to other studies that present exposure results for a limited number of locations, the procedure described in this paper represents a step forward for the comprehensive characterisation of territories, irrespective of their geographic location, that will contribute to improve building design even in locations where there are no or incomplete climatic records. Moreover, the results of this procedure may indeed facilitate the establishment of policy guidelines and requirements for water tightness of building enclosures when exposed to different exposure levels.

Acknowledgements

These results were obtained from data provided by the Xunta of Galicia, Generalitat of Catalonia and Junta of Andalusia. This work was partially financed by the Spanish Ministry of Science and Innovation co-financed with FEDER funds under the Research Project BIA2012-31609. We also recognise José Joaquín Martínez Soto for his help in the data collection and processing.

References

AEMET, 2013. Spanish Meteorological Agency. *http://www.aemet.es/es/serviciosclimaticos/vigilancia_clima/* [Last Accessed 22.01.2014]

Akingbade, F.O.A., 2004. Estimation of driving rain index for Nigeria. Architectural Science Review 47(2),103-106. (doi:10.1080/00038628.2004.9697032).

Bansal, R., Bati, T.S., Kothari, D.P., 2002. On Some of the Design Aspects of Wind Energy Conversion Systems. Energy Conversion and Management 43(16), 2175–2187 (doi:10.1016/S0196-8904(01)00166-2).

Blocken, B., Abuku, M., Nore, K., Briggen, P.M., Schellen, H.L., Thue, J.V., Roels, S., Carmeliet, J., 2011. Intercomparison of wind-driven rain deposition models based on two case studies with full-scale measurements. Journal of Wind Engineering and Industrial Aerodynamics 99(4), 448–459. (doi:10.1016/j.jweia.2010.11.004).

Blocken, B., Carmeliet, J., 2004. A review of wind-driven rain research in building science. J. Wind Eng. Ind. Aerodyn. 92(13), 1079–1130. (doi:10.1016/j.jweia.2004.06.003)

Blocken, B., Carmeliet, J., 2007. On the error associated with the use of hourly data in wind-driven rain calculations on building facades. Atmospheric Environment 41(11), 2335-2343. (doi:10.1016/j.atmosenv.2006.11.014).

Blocken B, Carmeliet J. 2008. Guidelines for the required time resolution of meteorological data for wind-driven rain calculations on buildings. Journal of Wind Engineering and Industrial Aerodynamics 96(5), 621-639. (doi: 10.1016/j.jweia.2008.02.008).

Blocken, B., Derome, J., Carmeliet, J., 2013. Rainwater runoff from building facades: A review. Building and Environment 60, 339-361. (doi:10.1016/j.buildenv.2012.10.008).

Blocken, B., Stathopoulus, T., Carmeliet, J., Hensen, J.L.M., 2011. Application of computational fluid dynamics in building performance simulation for the outdoor environment: an overview. Journal of Building Performance Simulation, 4(2), 157-184. (doi:10.1080/19401493.2010.513740).

BSI, 1992. BS 8104 Code of practice for assessing exposure of walls to wind-driven rain. British Standards Institution.

Carll, C., 2001. Rainwater intrusion in light-frame building walls. Second annual conference on durability and disaster mitigation in woodframe housing. Forest Products Society, 33-40, Madison, WI, USA.

Chand, I., Bhargava, P.K., 2002. Estimation of driving rain index for India. Building and Environment 37, 549-554. (doi:10.1016/S0360-1323(01)00057-9)

Cornick, S.M., Lacasse, M.A., 2005. A review of climate loads relevant to assessing the watertightness performance of walls, windows, and wall-window interfaces. Journal of ASTM International 2(10), 1-16. (doi:10.1520/JAI12505).

Del Coz, J.J., Rabanal, F.P., García, P.J., Domínguez, J., Rodríguez, B., Pérez, J.M., 2013. Hygrothermal properties of lightweight concrete: Experiments and numerical fitting study. Construction and Building Materials 40, 543-555. (doi: 10.1016/j.conbuildmat.2012.11.045)

Franke, L., Schumann, I., van Hees, R., van der Klugt, L., Naldini, S., Binda, L., Baronio, G., van Valen, K., Mateus, J., 1998. Damage atlas: classification and analyses of damage patterns found in brick masonry. European Commission Research report nr 8, vol 2. Fraunhofer IRB Verlag.

Generalitat of Catalonia, 2013. Meteorological Service of Catalonia. Catalonia, Spain. *http://www20.gencat.cat/portal/site/meteocat/* [Last accessed 22.01.2014].

Giarma, C., Aravantinos, D., 2011. Estimation of building components' exposure to moisture in Greece based on wind, rainfall and other climatic data. J. Wind Eng. Ind. Aerodyn. 99, 91-102. (doi: 10.1016/j.jweia.2010.12.001)

Haverinen-Shaughnessy, U., 2007. Moisture as a source of indoor air contamination. EnVIE Conference on Indoor Air Quality and Health for EU Policy, Helsinki.

Henriques, F.M.A., 1992. Quantification of wind-driven rain. An experimental approach. A general review on driven rain and details of an experiment in Portugal to supplement existing research results in Norway, the UK and elsewhere. Building Research and Information 20(5), 295-297. (doi: 10.1080/09613219208727227).

Hensen, J.L.M., Lamberts, R., 2011. Building Performance Simulation for Design and Operation. Spon Press, Abingdon.

Hoppestad, S., 1955. Slagregn i Norge (*Driving rain in Norway, in Norwegian*). Norwegian Building Research Institute Report no. 13, Oslo.

IDAE, 2009. Wind Atlas of Spain. Institute for Energy Diversification and Saving. Government of Spain. *http://atlaseolico.idae.es/index.php?idioma=EN* [Last accessed 22.01.2014].

ISO, 2009. Hygrothermal performance of buildings — Calculation and presentation of climatic data Part 3: Calculation of a driving rain index for vertical surfaces from hourly wind and rain data. ISO 15927-3.

Junta of Andalusia, 2013. Department of Agriculture, Fisheries and Environment. Andalusia, Spain. *http://www.juntadeandalucia.es/medioambiente/servtc5/WebClima/* [Last accessed 22.01.2014].

Kerr, D., 2004. Keeping walls dry. Canada Montage and Housing Corporation, Ottawa.

Kottek, M., Grieser, J., Beck, C., Rudolf, B., Rubel, F., 2006. World map of the Köppen-Geiger climate classification updated. Meteorol. Z. 15, 259-63. (doi: 10.1127/0941-2948/2006/0130)

Kubilay, A., Derome, D., Blocken, B., Carmeliet, J., 2013, CFD simulation and validation of wind-driven rain on a building façade with an Eulerian multiphase model. Building and Environment 61, 69-81. (doi:10.1016/j.buildenv.2012.12.005)

Kvande, T., Lisø, K.R., 2009. Climate adapted design of masonry structures. Building and Environment 44(12), 2442-2450. (doi:10.1016/j.buildenv.2009.04.007)

Lacy, R.E., 1965. Driving-rain maps and the onslaught of rain on buildings. Proceedings of RILEM/CIB symposium on moisture problems in buildings, Helsinki.

Lacy, R. E., 1971. An Index of Exposure to Driving Rain. Building Research Station, Digest No. 127, Garston, United Kingdom.

Lacy, R.E., 1977. Climate and Building in Britain. Her Majesty's Stationery Office, London.

Lacy, R.E., Shellard, H.C., 1962. An index of driving rain. The Meteorological Magazine 1080, 177-84.

Pérez, J.M., Domínguez, J., Rodríguez, B., del Coz, J.J., Cano, E., 2012. Estimation of the exposure to driving rain in Spain from daily wind and rain data. Building and Environment 57, 259-70. (doi:10.1016/j.buildenv.2012.05.010)

Pérez, J.M., Domínguez, J., Cano, E., del Coz, J.J., Navarro, A., 2013a. Global analysis of the exposure to water penetration in Chilean building façades. Building and Environment 70, 284-297.

Pérez, J.M., Domínguez, J., Rodríguez, B., del Coz, J.J., Cano, E., 2013b. Combined use of wind-driven rain and wind pressure to define water penetration risk into building façades: the Spanish case. Building and Environment 64, 46-56. (doi:10.1016/j.buildenv.2013.03.004)

Pérez, J.M., Domínguez, J., Rodríguez, B., del Coz, J.J., Cano, E., 2013c. Review and improvement of the water tightness degree required by the CTE DB-HS1 for building façades [in Spanish]. Informes de la Construcción (accepted 09.10.2013).

Prior, M.J., 1985. Directional driving rain indices for the United Kingdom – computation and mapping. Building Research Establishment, Garston.

Sahal, N., 2006. Proposed approach for defining climate regions for Turkey based on annual driving rain index and heating degree-days for building envelope design. Building and Environment 41, 520-6. (doi:10.1016/j.buildenv.2005.07.004).

Sahal, A.N., Lacasse, M.A., 2004. Experimental assessment of water penetration and entry into siding-clad wall specimen. Internal Report No. 862, National Research Council Canada, Ottawa. (doi: irc_id:16429).

Sanders, C., 1996. Heat, air and moisture transfer in insulated envelope parts: Environmental conditions, International Energy Agency, Annex 24, Final report, vol. 2, Leuven.

Straube, J., Burnett, F.P., 1999. Rain control and design strategies. Journal of Thermal Envelope and Building Science 23, 41–56. (doi: 10.1177/109719639902300105).

Straube, J.F., Burnett, E.F.P., 2000. Simplified Prediction of Driving Rain Deposition. Proceedings of International Building Physics Conference, pp. 375-382, Eindhoven.

Tang, W., Davidson, C.I., Finger, S., Vance, K., 2004. Erosion of limestone building surfaces caused by wind-driven rain. 1. Field measurements. Atmospheric Environment 38(33), 5589-5599. (doi:10.1016/j.atmosenv.2004.06.030)

Waldum, A.M., 1993. Restoration of masonry facades, renders and final coats in a severe climate. Composition and durability of old rendering mortars described and suggestions made for the composition of coating system for old masonry walls in severe climate. Building Research & Information, 21(1), 51-55. (doi:10.1080/09613219308727255).

WHO, 2011. Environmental burden of disease associated with inadequate housing. Methods for quantifying health impacts of selected housing risks in the WHO European Region. World Health Organization, Copenhagen.

WMO, 2008. Guide to Meteorological Instruments and Methods of Observation. WMO-No 8. World Meteorological Organization, Geneva.

Xunta of Galicia, 2013. Department of environment, territory and infrastructures. Galicia, Spain. *http://www.meteogalicia.es/* [Last accessed 22.01.2014].

List of tables

Table 1.

Comparison of terrain coverage from previous studies in Spain (Pérez et al., 2012, 2013b, 2013c) and the coverage of the current work.

	Spain		**Galicia**		**Catalonia**		**Andalusia**	
	Number of sites analysed	**Coverage (results/km^2)**	**Number of sites analysed**	**Coverage (results/km^2)**	**Number of sites analysed**	**Coverage (results/km^2)**	**Number of sites analysed**	**Coverage (results/km^2)**
Previous studies	80	1/6,308	5$^{(*)}$	1/5,915	5$^{(*)}$	1/6,420	12$^{(*)}$	1/7,272
Current work	-	-	80	1/370	147	1/218	166	1/525

$^{(*)}$ *Sites included within the 80 considered nationwide.*

Table 2.

Weather stations in Galicia with a risk index of water penetration greater than 0.4 *(31 of the 80 total stations)*.

Location	Latitude (DD)	Longitude (DD)	Altitude (m)	Years considered	maDRI (m^2/s)	daDRI (m^2/s)	Mean wind pressure (Pa)	$DRWP_a$ (Pa)	RIWP
Muralla (Lousame)	42.7601	-8.8475	80	2002-2012	18.8	22.5	29.1	37.2	1.21
Xesteiras (Cuntis)	42.6337	-8.5632	159	2011-2012	15.2	18.2	28.1	35.9	1.04
Punta Candeira (Cedeira)	43.6612	-8.0555	18	2004-2012	6.9	8.2	36.5	46.7	0.92
A Gandara	43.0126	-9.0055	480	2009-2012	9.7	11.5	24.5	31.3	0.77
Rio do Sol (Coristanco)	43.1903	-8.7609	140	2009-2012	9.9	11.8	21.4	27.4	0.72
Serra do Faro (Rodeiro)	42.6501	-7.9507	636	2006-2012	8.9	10.6	22.1	28.2	0.70
Malpica	43.3217	-8.8104	5	2006-2012	5.2	6.2	24.6	31.4	0.63
Pereira (Forcarei) [(1)]	42.5925	-8.3497	592	2006-2012	8.5	10.1	18.6	23.7	0.62
Olas (Mesia) [(1)]	43.1135	-8.2735	420	2005-2012	8.0	9.5	18.6	23.7	0.60
Serra da Falaidora	43.5833	-7.7832	601	2006-2012	7.8	9.2	18.7	23.8	0.60
Rebordelo (Cotobade) [(1)]	42.4665	-8.4657	660	2006-2012	8.4	9.9	16.2	20.6	0.58
Fornelos de Montes	42.3402	-8.4527	800	2003-2012	9.4	11.1	13.0	16.5	0.58
Marco da Curra (Monfero)	43.3256	-8.0530	340	2002-2012	8.1	9.7	16.7	21.2	0.58
Salvora	42.4727	-9.0100	73	2006-2012	6.6	7.8	20.0	25.4	0.58
Xares (A Veiga)	42.2549	-7.0246	893	2007-2012	5.9	6.9	21.0	26.7	0.58
Cabeza de Manzaneda	42.3108	-7.2352	661	2007-2012	3.6	4.2	23.0	29.4	0.57
Santiago airport [(2)]	42.8877	-8.4108	370	> 30 years	7.8	11.1	11.9	15.1	0.56
Lira	42.7994	-9.1267	37	2010-2012	4.0	4.7	21.5	27.5	0.54
Castro Vicaludo (Oia)	42.0023	-8.8756	35	2004-2012	5.8	6.9	18.9	24.1	0.54
Ons (Bueu)	42.3199	-8.7901	4	2005-2012	5.7	6.7	18.0	22.9	0.51
Ancares (Cervantes)	42.8709	-7.0630	600	2002-2012	6.6	7.8	15.3	19.4	0.49
Fragavella (Abadin)	43.3661	-7.4715	510	2004-2012	7.7	8.5	12.7	16.0	0.48
Lardeira (Carballeda de Valdeorras)	42.3778	-6.8809	631	2007-2012	4.1	4.8	18.4	23.4	0.47
Burela	43.3904	-7.2126	80	2006-2012	5.5	6.5	16.3	20.7	0.47
Sambeixo [(1)]	42.8676	-7.9275	595	2002-2012	5.0	5.9	16.2	20.6	0.46
Corón (Vilanova de Arousa)	42.5629	-8.8282	8	2002-2012	6.0	7.1	13.6	17.3	0.45
Camarinas	43.1285	-9.1854	20	2009-2012	3.3	3.9	16.8	21.3	0.42
Castro R. de Lea (De Rei) [(1)]	43.2061	-7.3995	430	2010-2012	3.5	4.1	16.2	20.6	0.42
Penedo do Galo (Viveiro) [(1)]	43.5973	-7.5017	19	2006-2012	5.0	5.9	14.0	17.7	0.41
Vigo airport [(2)]	42.2394	-8.6238	261	> 30 years	6.4	8.2	8.3	9.8	0.41
Alto do Rodicio (Maceda)	42.2728	-7.6504	577	2002-2012	5.6	6.6	12.0	15.2	0.40

[(1)] Wind velocity estimated from wind maps;[(2)] Results obtained from previous studies that used daily records (Eqs. 5 and 7 are not used to derive daDRI and $DRWP_a$ values).

Table 3.

Weather stations in Catalonia with a risk index of water penetration greater than 0.15 *(16 of the 147 total stations).*

Location	Latitude (DD)	Longitude (DD)	Altitude (m)	Years considered	maDRI (m^2/s)	daDRI (m^2/s)	Mean wind pressure (Pa)	$DRWP_a$ (Pa)	RIWP
Portbou	42.4265	3.1581	27	1999-2011	4.5	5.1	38.7	36.5	0.70
Barcelona airport [(2)]	41.2936	2.0700	4	> 30 years	2.4	2.7	11.3	12.1	0.25
El Perello	40.8751	0.7126	150	1999-2011	2.3	2.5	13.0	11.9	0.24
Torroella de Fluviá [(1)]	42.1753	3.0401	9	2001-2011	2.6	2.9	11.9	10.9	0.24
Castello d'Empuries [(1)]	42.2585	3.0747	4	2001-2011	2.5	2.8	11.9	10.9	0.23
Parlavá [(1)]	42.0217	3.0318	27	2001-2003	2.8	3.1	10.0	9.1	0.22
Ventalló [(1)]	42.1504	3.0249	27	2001-2011	2.6	2.8	10.0	9.1	0.21
Veciana	41.6565	1.4886	562	1997-1998	1.8	1.9	10.9	9.9	0.20
Blancafort [(1)]	41.1367	1.0960	430	2001-2011	1.8	2.0	10.0	9.1	0.19
Reus airpot [(2)]	41.1497	1.1788	71	> 30 years	1.7	1.7	11.4	9.1	0.18
Espolla, Les Alberes [(1)]	42.2324	3.0022	94	2001-2011	2.5	2.7	8.3	7.4	0.18
Torroella de Montgrí [(1)]	42.0436	3.1241	30	2001-2011	2.4	2.6	8.3	7.4	0.18
Botarell	41.1354	0.9904	195	1999-2003	1.9	2.1	8.6	7.7	0.17
Nulles [(1)]	41.2506	1.2958	232	2001-2011	2.0	2.2	8.3	7.4	0.17
Fornells [(1)]	41.9320	2.8123	101	2001-2011	2.4	2.7	6.7	5.9	0.16
Begur	41.9533	3.2079	198	1997-2002	1.8	2.0	7.9	7.1	0.16

[(1)] Wind velocity estimated from wind maps;[(2)] Results obtained from previous studies that used daily records (Eqs. 6 and 8 were not used to derive daDRI and $DRWP_a$ values).

Table 4.

Weather stations in Andalusia with a risk index of water penetration greater than 0.2 (*12 of the 166 total stations*).

Location	Latitude (DD)	Longitude (DD)	Altitude (m)	Years considered	daDRI (m^2/s)	$DRWP_a$ (Pa)	RIWP
Tarifa[(1)]	36.0152	-5.5975	32	> 30 years	5.8	55.0	1.03
Moguer	37.2773	-6.8365	50	2003-2012	0.3	30.7	0.56
Jerez de la Frontera airport[(1)]	36.7505	-6.0558	27	> 30 years	3.7	20.1	0.40
Cadiz[(1)]	36.5011	-6.2566	1	> 30 years	3.1	19.3	0.38
San Roque, Sotogrande	36.2099	-5.3841	1	2002-2011	7.9	7.5	0.37
Morón de la Frontera[(1)]	37.1583	-5.6158	87	> 30 years	3.2	18.9	0.37
Almería airport[(1)]	36.8463	-2.3569	21	> 30 years	1.0	17.8	0.33
Grazalema (EMA)	36.7598	-5.3669	913	2010-2011	2.7	14.5	0.29
Sevilla airport[(1)]	37.4166	-5.8791	34	> 30 years	2.7	13.0	0.26
La Línea de la Concepción	36.1631	-5.3456	3	2002-2011	5.0	7.2	0.26
Córdoba airport[(1)]	37.8441	-4.8461	90	> 30 years	2.4	11.5	0.23
Huelva[(1)]	37.2800	-6.9097	19	> 30 years	2.2	11.1	0.22

[(1)] *Results obtained from daily records in previous studies.*

Figure captions

Fig. 1. Map of Spain illustrating the location of the three regions of interest for analysis and the locations in these regions considered in previous studies (Pérez et al., 2012, 2013b, 2013c). *Darker colours represent higher altitudes.*

Fig. 2. Scheme for the combination of the data sources to undertake a detailed analysis of WDR and DRWP exposures.

Fig. 3. Best-fit linear *maDRI-daDRI* relationships derived from the results of previous studies (Pérez et al., 2012).

Fig. 4. Best-fit linear *$DRWP_a$-mean wind pressure* relationships derived from the results of previous studies (Pérez et al., 2013b, 2013c).

Fig. 5. Integration of climatic data, wind maps and fitting relationships using the procedure described in this study.

Fig. 6. *daDRI* isopleth map of Galicia, Spain (m^2/s).

Fig. 7. *$DRWP_a$* isopleth map of Galicia, Spain (Pa).

Fig. 8. *daDRI* isopleth map of Catalonia, Spain (m^2/s).

Fig. 9. *$DRWP_a$* isopleth map of Catalonia, Spain (Pa).

Fig. 10. *daDRI* isopleth map of Andalusia, Spain (m^2/s).

Fig. 11. *$DRWP_a$* isopleth map of Andalusia, Spain (Pa).

Fig. 12. Best-fit linear *WDR-$DRWP_a$* relationships in Galicia, Catalonia and Andalusia.

Fig. 13. Risk index of water penetration in building façades for the three Spanish regions.

Figure 1

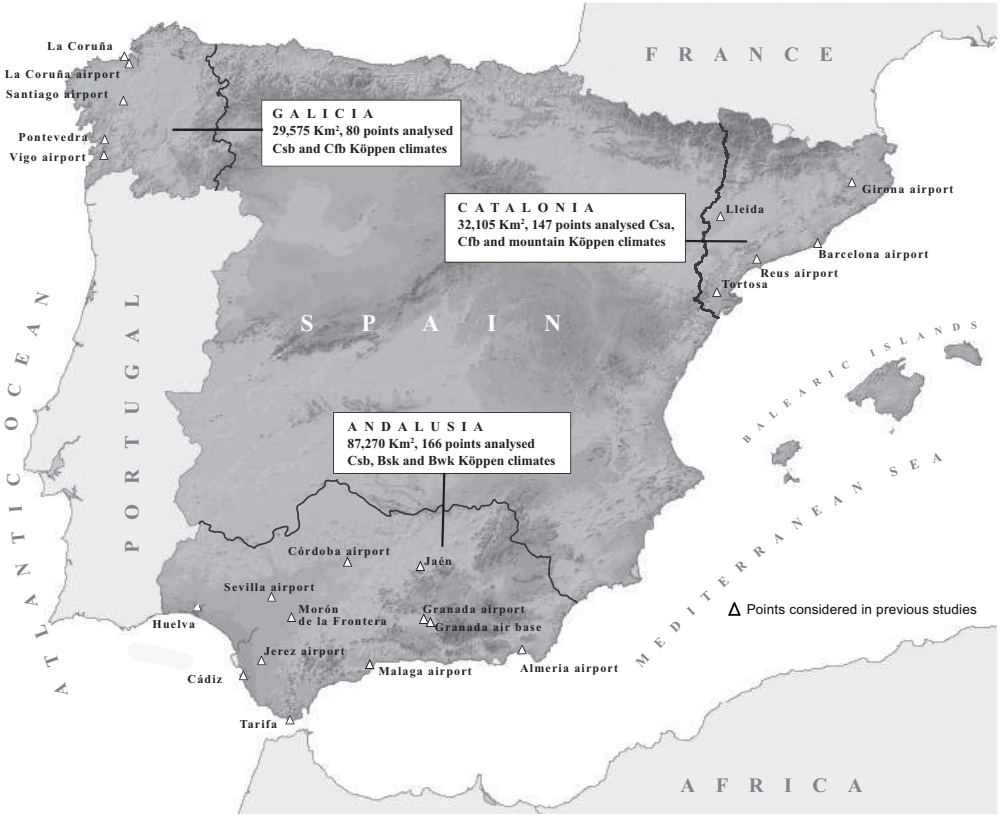

Figure 1. Map of Spain illustrating the location of the three regions of interest for analysis and the locations in these regions considered in previous studies (Pérez et al., 2012, 2013b, 2013c). *Darker colors represent higher altitudes.*

Figure 2

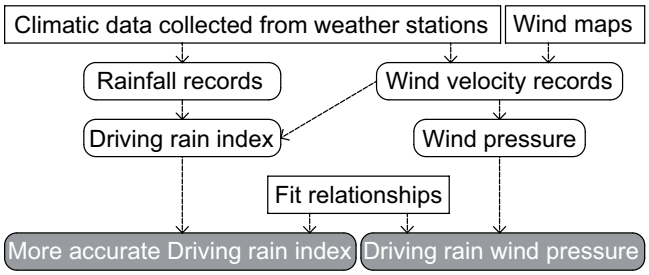

Figure 2. Scheme for the combination of data sources to undertake a detailled analysis of WDR and DWRP exposures.

Figure 3

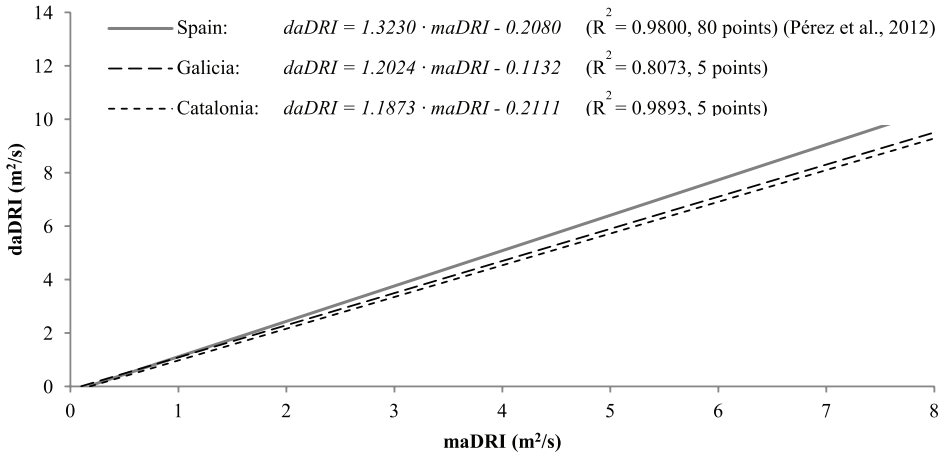

Figure 3. Best fit-linear *maDRI-daDRI* relationships derived from the results of previous studies (Pérez et al., 2012).

Figure 4

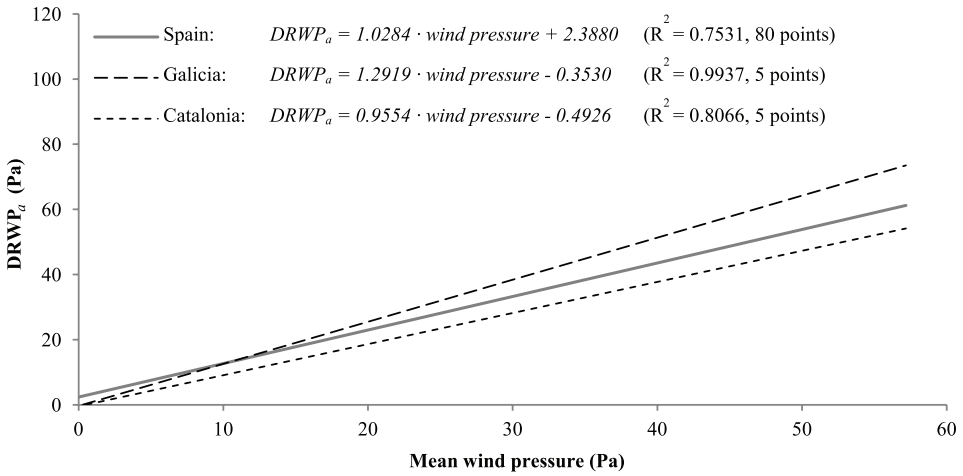

Figure 4. Best fit-linear *$DRWP_a$ - mean wind pressure* relationships derived from the results of previous studies (Pérez et al., 2013b, 2013c).

Figure 5

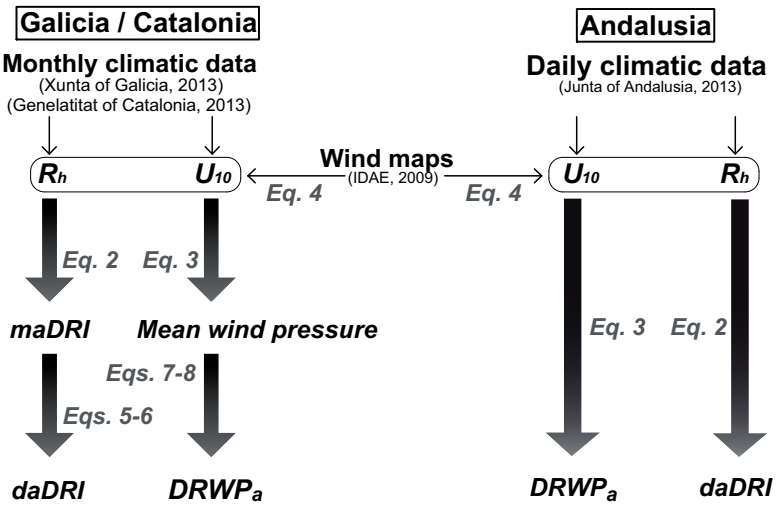

Figure 5. Integration of climatic data, wind maps and fitting relationships using the procedure described in this study.

Figure 6

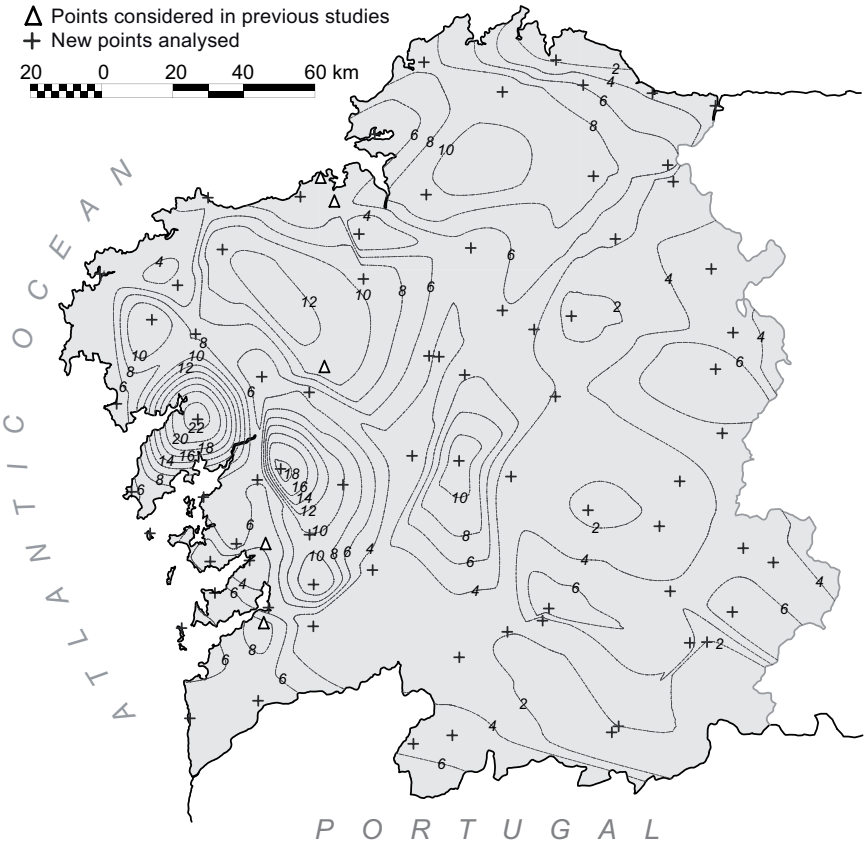

Figure 6. *daDRI* isopleth map of Galicia, Spain (m^2/s).

Figure 7

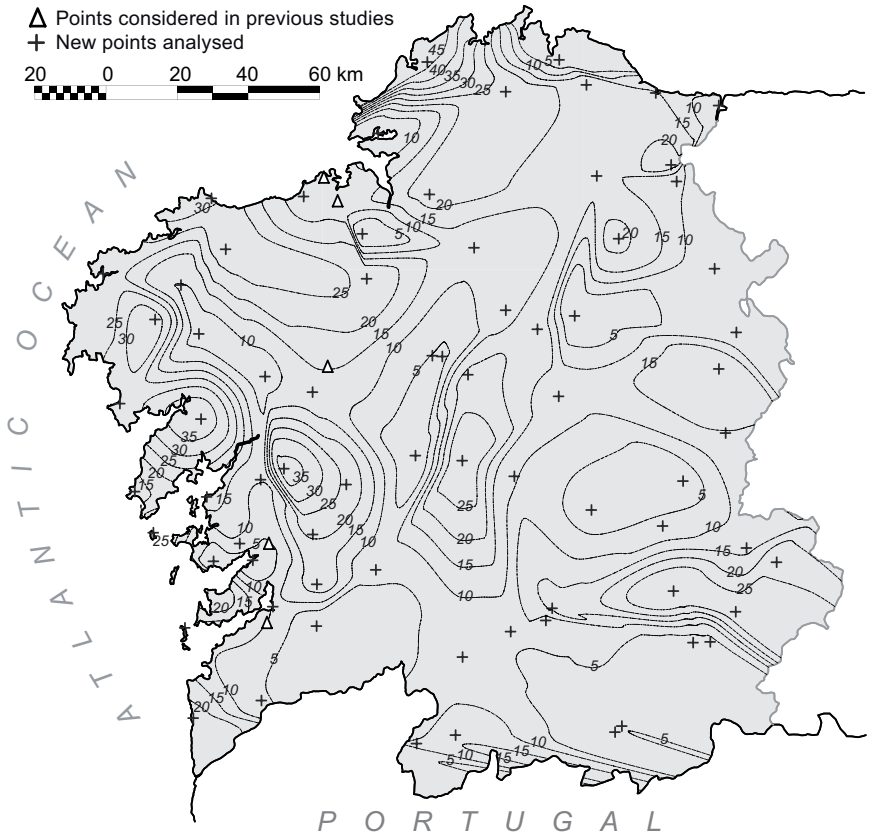

Figure 7. *DRWP*$_a$ isopleth map of Galicia, Spain (Pa).

Figure 8

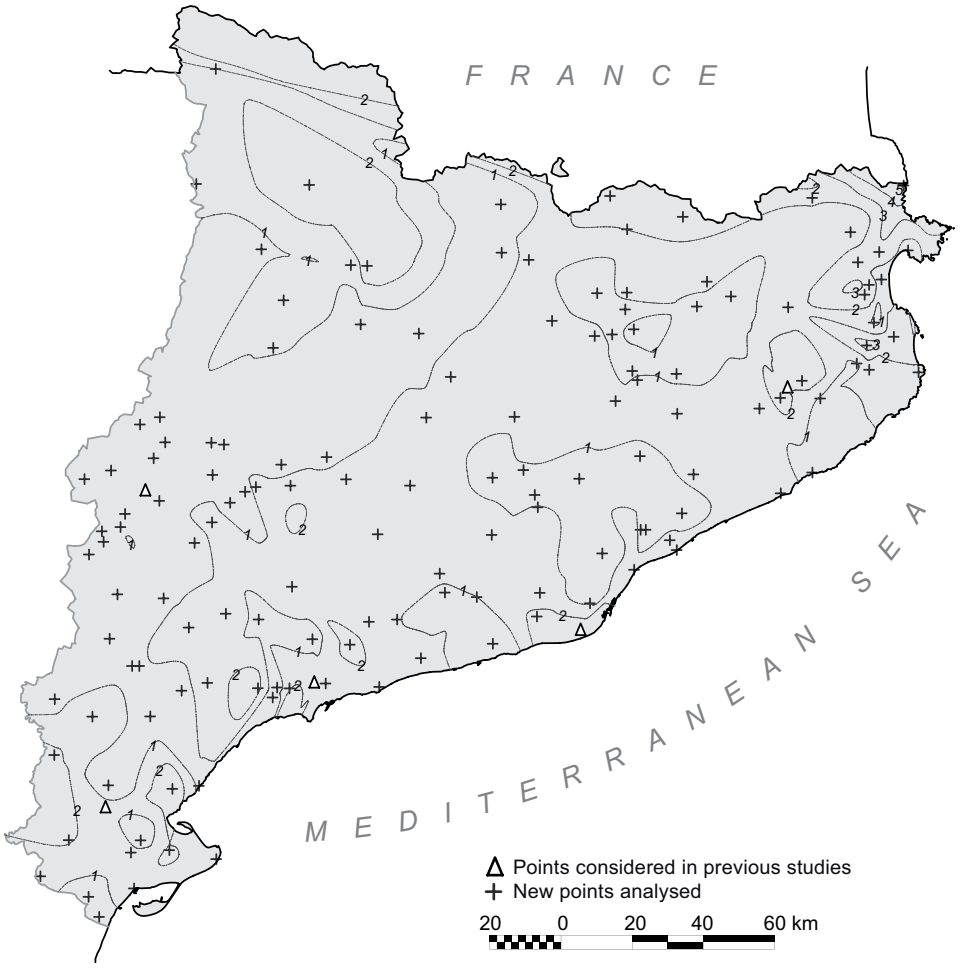

Figure 8. *daDRI* isopleth map of Catalonia, Spain (m^2/s).

Figure 9

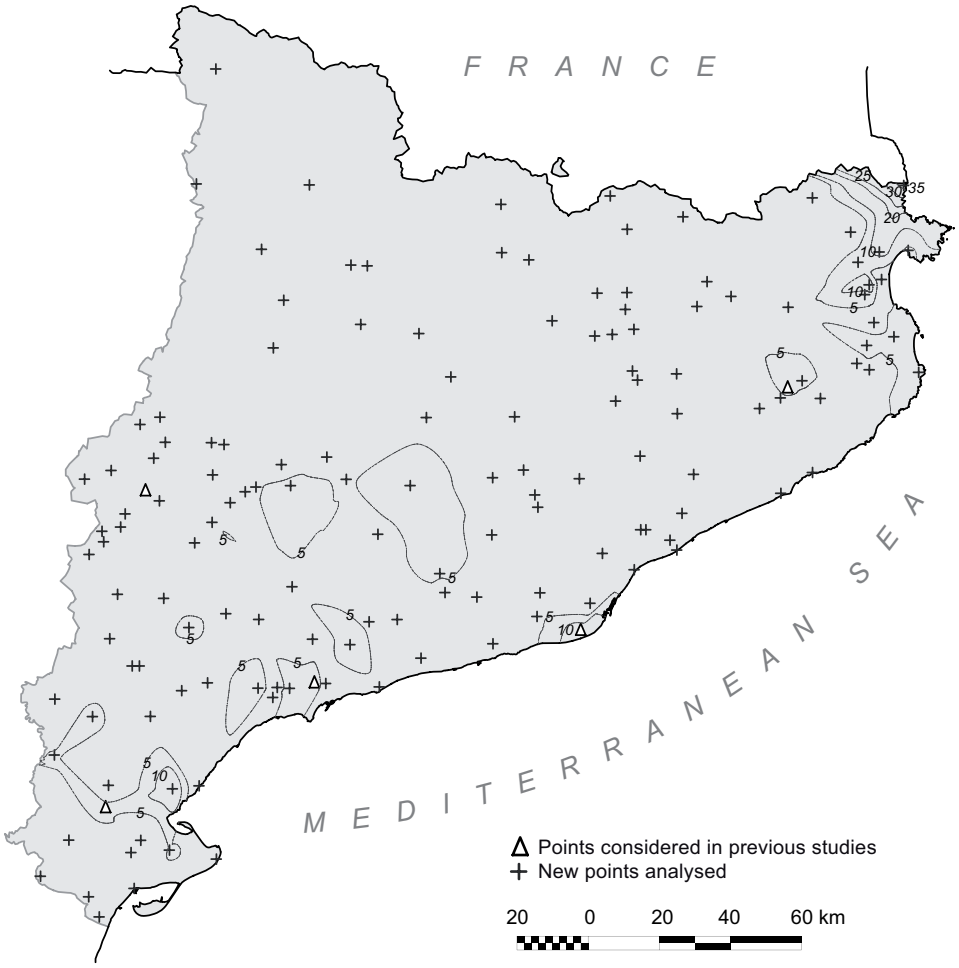

Figure 9. *DRWP*$_a$ isopleth map of Catalonia, Spain (Pa).

Figure 10

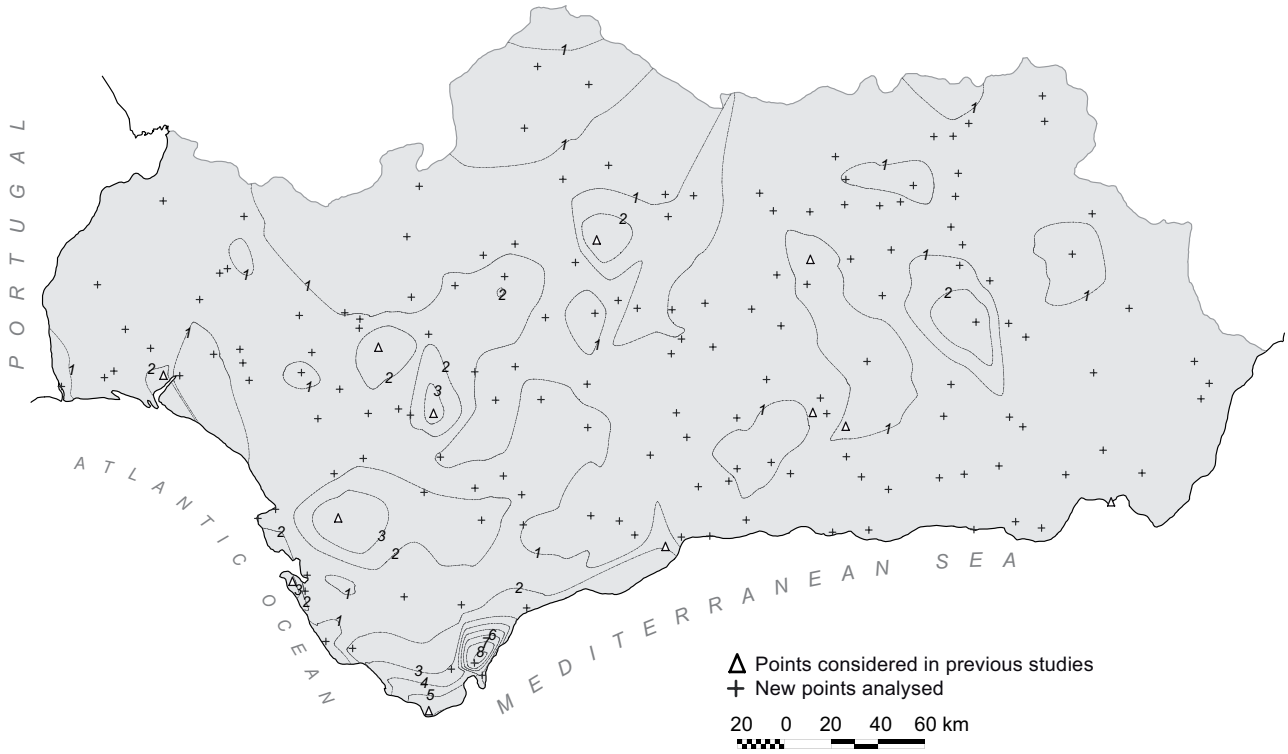

Figure 10. *daDRI* isopleth map of Andalusia, Spain (m^2/s).

Figure 11

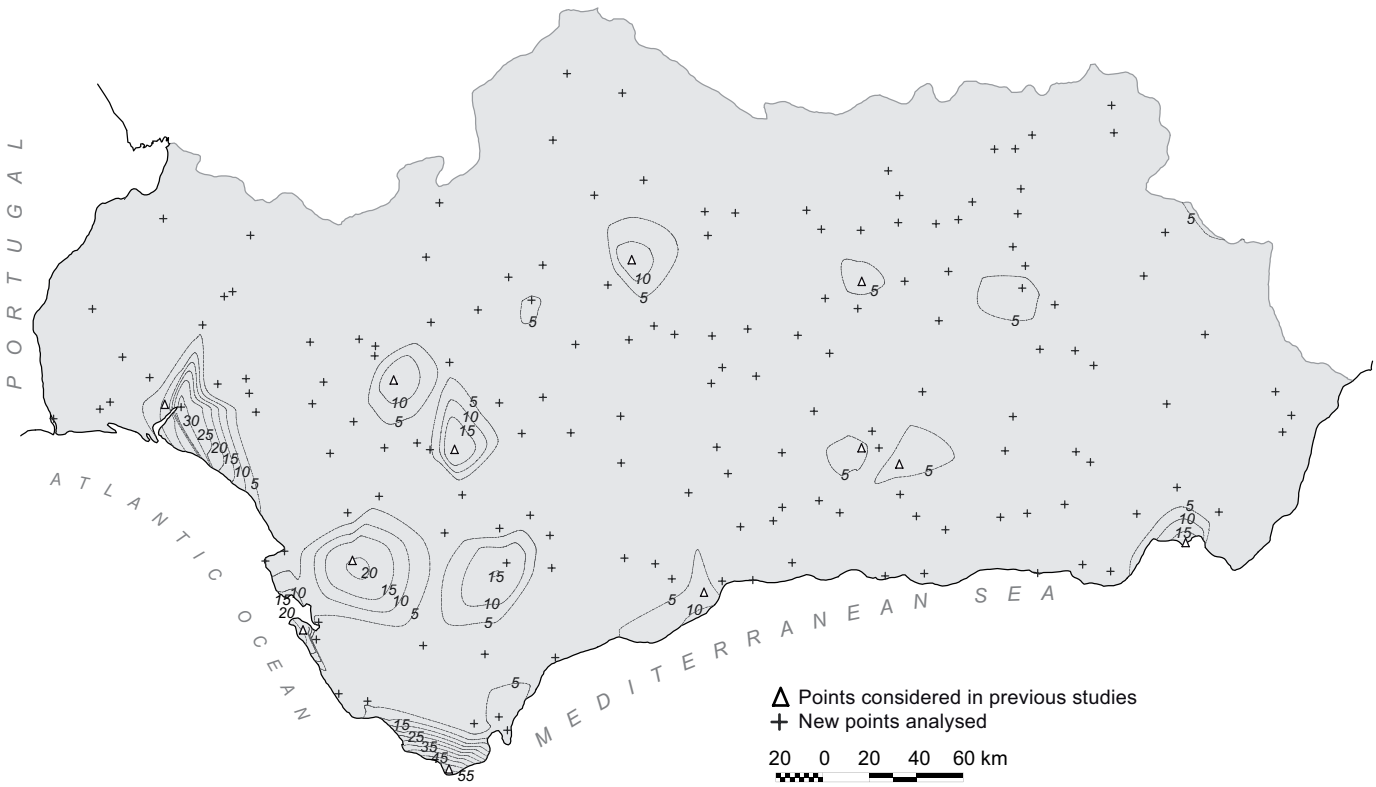

Figure 11. *DRWP*$_a$ isopleth map of Andalusia, Spain (Pa).

Figure 12

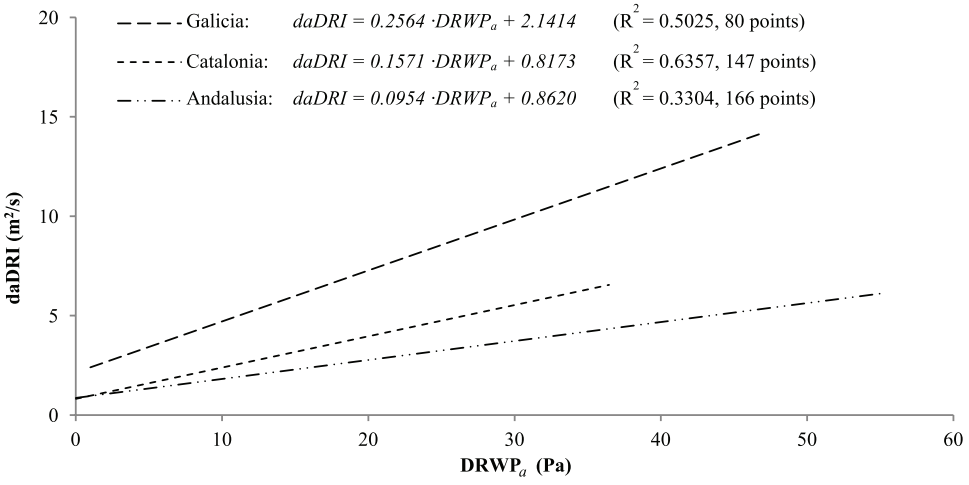

Figure 12. Best fit-linear *WDR-DRWP$_a$* relationships in Galicia, Catalonia and Andalusia.

Figure 13

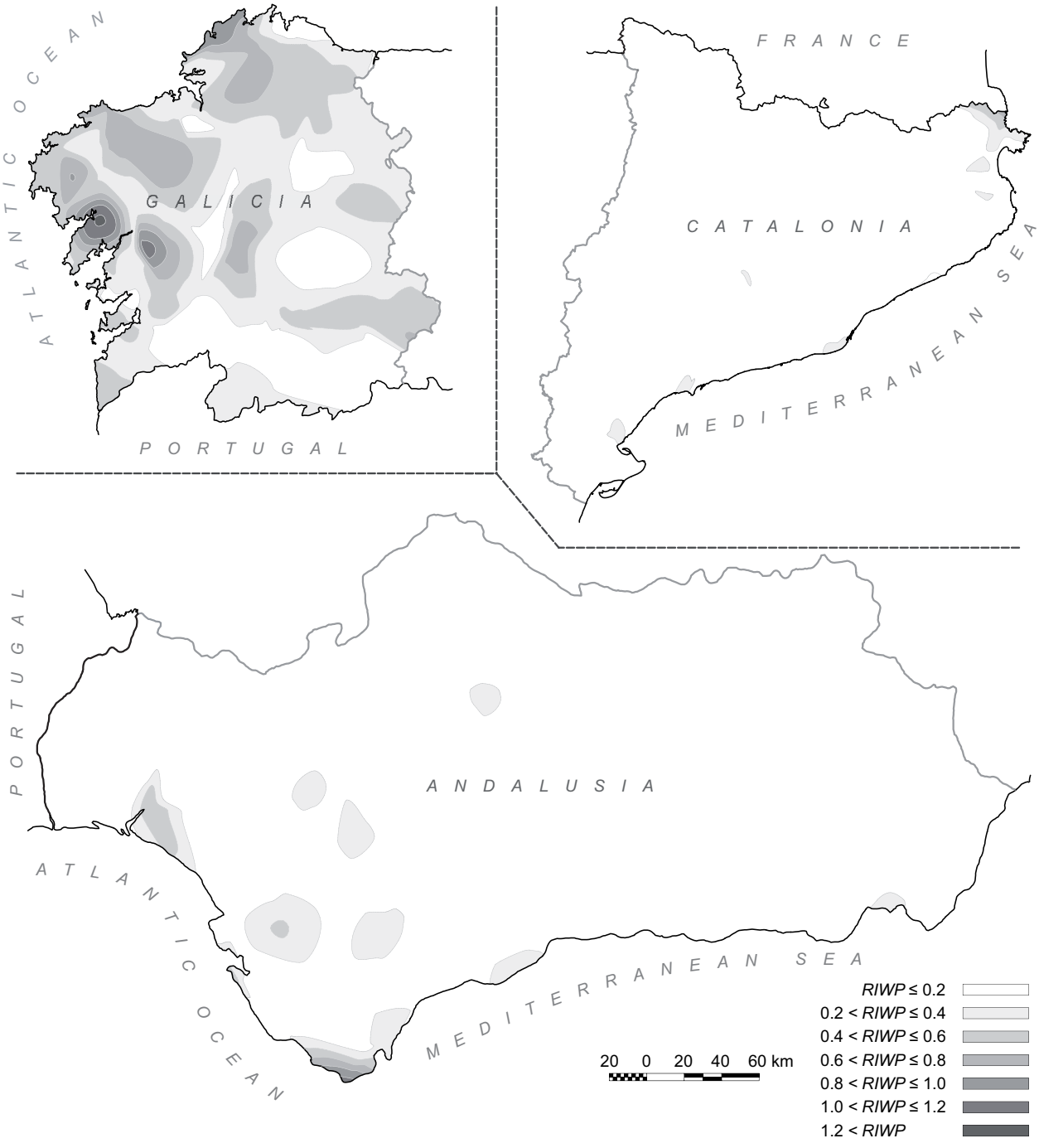

Figure 13. Risk index of water penetration in building façaces for the three Spanish regions.